Electrical and thermal properties of dense $Ce_{1-x}RE_xO_{2-\delta}$ electrolyte using low-temperature sinterable powder (0 ≤ x ≤ 0.2, RE=Y, Sm, Gd)

Eisaku Suda, Bernard Pacaud, Yvan Montardi*, Masashi Mori**, Yasuo Takeda***

R&D Department, ANAN KASEI Co.,Ltd., 210-51, Ohgata, Anan, Tokushima 774-0022, Japan
Tel:+81-884-27-3211, Fax:+81-884-27-2922, E-mail: eisaku.suda@ap.rhodia.com
*Aubervilliers Research Center, Rhodia Electronics and Catalysis, 52 rue de la Haie-coq-F-93308 Aubervilliers Cedex, France
**Energy Materials Science Department, Central Research Institute of Electric Power Industry, 2-6-1 Nagasaka, Yokosuka, Kanagawa 240-0196
***Department of Chemistry, Faculty of Engineering, Mie University, 1515 Kamihama, Tsu, 514-0008, Japan

The low-temperature sinterable rare earth metal (RE)-doped cerium oxide powders ($Ce_{1-x}RE_xO_{2-\delta}$, 0 ≤ x ≤ 0.2, RE=Y, Sm, Gd) have been synthesized through a newly-devised heat-treatment process in the coprecipitation method, and their sintering, electrical and thermal properties have been examined as electrolytes in the low-temperature solid oxide fuel cells. Sintering characteristics for all the samples were improved remarkably. Especially, their relative densities of $Ce_{0.9}Y_{0.1}O_{1.95}$ and $Ce_{0.9}Gd_{0.1}O_{1.95}$ powders reached approximately 94% at 1050°C for 2 h. Electrical conductivities and thermal expansion coefficients of the sintered samples were almost comparable to those by the ordinal coprecipitation method.
Key words: Cerium oxide, SOFC, Electrical conductivity, Thermal property Coprecipitation method, Electrolyte

1. INTRODUCTION

Solid oxide fuel cells (SOFC) have attracted a great deal of attention as a clean and efficient power source for generating electricity from a variety of fuels. Current SOFC designs mainly employ Y_2O_3 stabilized ZrO_2 (YSZ) as the electrolyte, and a typical operating temperature is around 1000°C. Recently, it is expected to apply SOFC to the main driving source in fuel cell vehicles and the auxiliary power unit (APU) [1]. From the viewpoint of the quick start and the use of metallic cell components, the operating temperature is being tried to decrease to low temperatures, 500-700°C. Ceria-based oxides at 800°C exhibit comparable oxide-ion conductivity to zirconia-based oxides at 1000°C [2,3]. Due to this high oxide-ion conductivities, ceria-based oxides are expected to be candidates for the electrolyte of low-temperature SOFC.

The low-temperature sinterable $Ce_{0.9}Gd_{0.1}O_{1.95}$ powders have been developed using a newly-devised heat-treatment process in the coprecipitation method [4]. This powder shows the lowest value in the reported sintering temperatures of $Ce_{0.9}Gd_{0.1}O_{1.95}$ powders [5]: A relative density ≥ 94%, where sintered ceramics can provide gastightness, is attained for this powder after heating at temperatures ≥ 1050°C for 2 h. The low-temperature sinterable electrolyte powders offer a large selection of conditions during the fabricating processes and a significant economic advantage due to an avoidance of the degradation by the chemical reaction. The aim of this study is to synthesize low-temperature sinterable $Ce_{1-x}RE_xO_{2-\delta}$ powders (x=0, 0.1 and 0.2, RE = Y, Sm and Gd) by the new coprecipitation method and to examine their sintering characteristics, electrical conductivity and thermal expansion coefficients (TEC) of these sintered samples.

2. EXRERIMENTAL

The low-temperature sinterable ceria powders were basically synthesized using the coprecipitation method [4]: The metal nitrate aqueous solutions as starting materials $Ce(NO_3)_3$ (99.9 %, Rhodia, France) and $Gd(NO_3)_3$ (99.9 %, Rhodia, France) were used. Concentrations of aqueous solutions of $Ce(NO_3)_3$ (ca. 2.5 mol/L), and $Gd(NO_3)_3$ (ca. 2.0 mol/L) were confirmed by inductively couple plasma (ICP) analysis. They were mixed in a selected proportion of Ce / Gd = 0.90 / 0.10 (mol ratio) and were then poured into a water solution of NH_4HCO_3 (extra pure regent, Wako Pure Chem. Ltd., Japan). After the homogeneous precipitate obtained by the coprecipitation method, the precipitate was stirred at 80°C for 3 h before filtration. The precipitate was dried and calcined at 700°C for 5 h in air. Then, the compositions of the calcined powders were confirmed by inductively coupled plasma (ICP) analysis again, and the obtained proportions of Ce and RE were in good agreement with those of the starting compositions within experimental error ≤ 2%. The main impurities in the doped CeO_2 powders were 3 ppm for CaO and 1 ppm for Fe_2O_3. SiO_2 and Al_2O_3, which have an influence on the sintering characteristics [6], were observed in the detection limit.

All the samples were analyzed by powdered X-ray diffractometry (XRD) (18 kW, Mac Science, M18XHF22) using monochromated CuKα radiation and a scintillation detector. Specific surface area, particle size and particle size distribution of the powders were measured in the same methods and conditions [4].

The density of the sintered specimens was determined from observed values of size and weight of the specimens. Relative density was derived using the theoretical value determined from the experimental lattice parameters and unit formula.

Electrical conductivities were measured by the four-terminal method [4], and linear thermal expansion coefficient (TEC) was measured using a Mac Science TD5000S system [7].

3. RESULTS AND DISCUSSION
3.1 Sintering characteristics

It was concluded that all the samples showed a single fluorite phase after 700°C for 5 h, since no peaks for other phases were observed in the XRD patterns. Lattice parameters, cell volume, theoretical densities, average particle size and surface area of prepared ceria powders calcined at 700°C for 5 h are summarized in Table I. These values were in good agreement with those by Hayashi et al. [8]

Figures 1(a), (b) and (c) show the relative densities of the doped ceria powder as a function of sintering temperature, where the holding time at the highest temperature is 2 h. Generally, an acceptable relative density of electrolyte for SOFC is ≥ 94%, and the shaded region in Figs. 1 indicates this. The broken line in Figs. 1 shows the relative density of pure CeO2 at the sintering temperature. The sintering characteristics of all the sample powders were improved; compared to those of the ordinal coprecipitation powders [5]. Improved sintering characteristics were evaluated from the subtraction of sintering temperature of the new coprecipitation powders from that of the ordinal coprecipitation ones, and the values (ΔT) are given in Table 1. In this case, the sintering temperatures, where the relative densities of the samples reached 94%, is used. The relative density of CeO$_2$ reached at approximately 94% at 1200°C for 2 h. For Y or Gd doping, the sintering characteristics enhanced with increasing the content up to 10 mol%, and then lowers. The relative density of Ce$_{0.9}$Y$_{0.1}$O$_{1.95}$ and Ce$_{0.9}$Gd$_{0.1}$O$_{1.95}$ was 94% at 1050°C for 2 h and these high sintering characteristics are one of the lowest in the reported sintering temperatures of doped ceria powders. On the other hand, sintering characteristics of Sm-doped cerias were lower than those of Y- or Gd-doped ones.

Specific surface area was used to evaluate primary particle size of the ceria powders. Figure 2 shows the
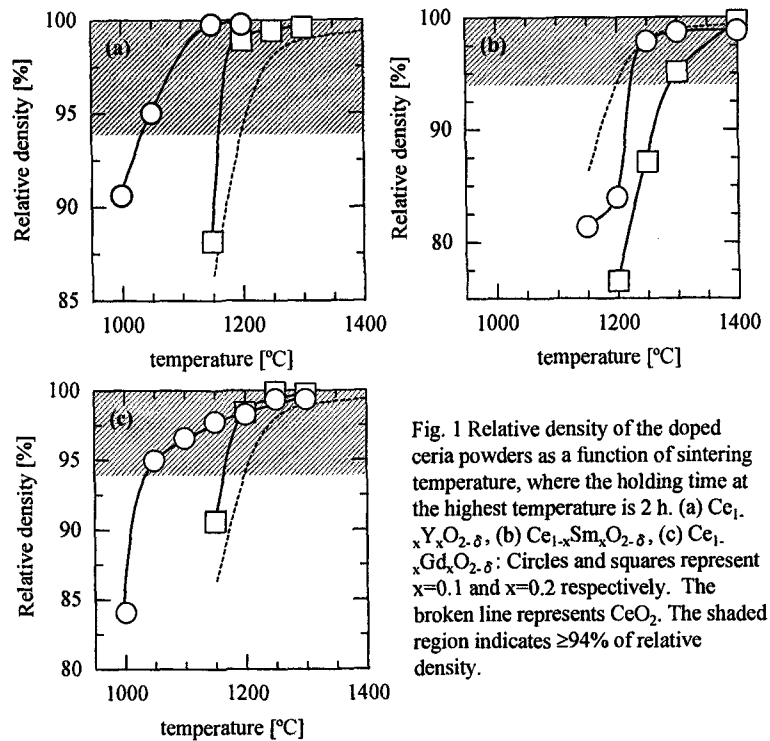

Fig. 1 Relative density of the doped ceria powders as a function of sintering temperature, where the holding time at the highest temperature is 2 h. (a) Ce$_{1-x}$Y$_x$O$_{2-\delta}$, (b) Ce$_{1-x}$Sm$_x$O$_{2-\delta}$, (c) Ce$_{1-x}$Gd$_x$O$_{2-\delta}$: Circles and squares represent x=0.1 and x=0.2 respectively. The broken line represents CeO$_2$. The shaded region indicates ≥94% of relative density.

specific surface area of the doped ceria powders clacined at 700°C for 5 h, as a function of dopant content. The specific surface area for all the samples had a tendency to increase with increasing dopant content. Thus, when the doped cerias are compared to the pure ceria, it is expected that it shows higher sintering characteristics. The results for Ce$_{1-x}$Y$_x$O$_{2-\delta}$ and Ce$_{1-x}$Gd$_x$O$_{2-\delta}$ agreed with the expectation. On the other hand, although Ce$_{1-x}$Sm$_x$O$_{2-\delta}$ powders have large specific surface area, the low sintering characteristics was observed.

Sintering characteristics of ceramic powders are strongly affected by the particle size distribution. Figure 3 shows the particle size distribution for the pure and doped ceria powders calcined at 700°C for 5 h. It is clear in Figs. 3 that a peak for the distribution is observed for CeO$_2$, Ce$_{0.9}$RE$_{0.1}$O$_{1.95}$ and Ce$_{1-x}$Sm$_x$O$_{2-\delta}$. On the other hand, two peaks for distribution are observed for Ce$_{0.8}$Y$_{0.2}$O$_{1.9}$ and Ce$_{0.8}$Gd$_{0.2}$O$_{1.9}$. Since the fine primary particles with high surface energy are agglomerated easily as second particles, the particle size distribution with two peaks is observed. It is known that pores are formed in the green body and will remain during sintering when many particles are strongly

Table I Lattice parameters, subtraction of sintering temperatures, theoretical densities, average particle size and specific surface area of prepared cerium powders calcined at 700°C for 5 h. The sintering temperatures, where the relative densities of samples reached 94%, were used.

| Sample	a (Å)	Cell volume (Å^3)	Theoretical density (g/cm^3)	Average particle size (μ m)	Spacific surface area (m^2/g)	ΔT (°C)
CeO$_2$	5.4078(6)	158.15	7.231	0.21	16.4	200
Ce$_{0.9}$Y$_{0.1}$O$_{1.95}$	5.4096(3)	158.30	6.976	0.18	39.9	250
Ce$_{0.8}$Y$_{0.2}$O$_{1.9}$	5.4097(4)	158.31	6.727	0.44	34.8	150
Ce$_{0.9}$Sm$_{0.1}$O$_{1.95}$	5.4209 (6)	159.30	7.189	0.21	21.1	150
Ce$_{0.8}$Sm$_{0.2}$O$_{1.9}$	5.4356(6)	160.60	7.140	0.20	22.3	100
Ce$_{0.9}$Gd$_{0.1}$O$_{1.95}$	5.4217(5)	159.37	7.214	0.22	30.0	250
Ce$_{0.8}$Gd$_{0.2}$O$_{1.9}$	5.4233(2)	159.51	7.208	3.34	37.9	150
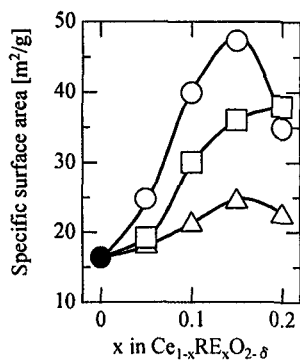
Fig.2 Specific surface area of the doped ceria powders as a function of dopant content. Open circles, open triangles and open squares represent $Ce_{1-x}Y_xO_{2-\delta}$, $Ce_{1-x}Sm_xO_{2-\delta}$ and $Ce_{1-x}Gd_xO_{2-\delta}$. Closed circle represent CeO_2.

Fig. 3 Particle size distribution of the doped ceria powders. Real lines, dotted lines and broken lines represent x=0, x=0.1 and x=0.2, respectively. (a) $Ce_{1-x}Y_xO_{2-\delta}$, (b) $Ce_{1-x}Sm_xO_{2-\delta}$, (c) $Ce_{1-x}Gd_xO_{2-\delta}$

aggregated [9]. So they will show lower sintering characteristics.

We reported that the low-temperature sintering characteristics of $Ce_{0.9}Gd_{0.1}O_{1.9}$ powder by the new precipitation method are related to a crystallization of the precipitates during the heat-treatment process at 80°C [4]. XRD patterns of the non heat-treatment precipitate showed an amorphous phase. On the other hand, XRD patterns of the heat-treatment precipitates showed the mixture of intermediate products such as $Ce(CO_3)_2O \cdot H_2O$ [10], $Ce_2O(CO_3)_2 \cdot H_2O$ [11], $Ce_2(CO_3)_2(OH)_2 \cdot H_2O$ [12] and $Ce_2(CO_3)_3 \cdot 8H_2O$ [13]. No differences of the XRD patterns were observed for all the ceria precipitates. Although Sm-doped samples showed the lowest sintering characteristics, the powders synthesized by the new coprecipitation method show higher sintering characteristics. In the case of $Ce_{0.9}Sm_{0.1}O_{1.95}$, when compared to those by the ordinal one, relative densities ≥ 94 % were observed to be 1250°C for 2 h for the new coprecipitation method and 1400°C for 2 h for the ordinal one.

3.2 Electrical and thermal properties

It is well known that ceria-based oxides show the formation of oxygen vacancies in the fluorite structure and a charge compensation of the Ce^{4+} to the Ce^{3+} ion occurs in reducing atmosphere at temperatures greater than ~550°C [14, 15]. Two serious problems remain to

be solved: (1) Although, at high oxygen partial pressures, ceria-based oxides show a purely oxide-ion conductor, the reduction of Ce^{4+} into Ce^{3+} ions causes the appearance of electronic conduction at high temperatures ≥ around 700°C in low oxygen partial pressures. (2) Since the ionic radius of Ce^{3+} ions (128.3 pm) is larger than that of Ce^{4+} ions (111 pm) on the cation-sites in the fluorite structure [16], the crystal lattice expands by charge compensation. In addition, the formation of oxygen vacancies also reduces Coulombic interactions between cations and anions; accordingly the crystal lattice expands. These phenomena cause a large isothermal expansion (reduced expansion) of cerium-based oxides.

Since a very small amount of transfer of Ce^{4+} into Ce^{3+} ions occur at temperatures ≤ 700°C even in a H_2 atmosphere, low-temperature operation of SOFC using CeO_2 electrolyte is appropriate with respect to inhibition of appearance of electronic conduction and large isothermal thermal expansion in low oxygen partial pressures.

Figure 4 shows the Arrhenius plots of electrical conductivity of the $Ce_{1-x}RE_xO_{2-\delta}$ samples with relative density of approximately 95%. The oxide-ionic conductivities of the present samples agree to those reported previously [2]. This suggests that the present samples are without impurities such as SiO_2, which inhibits oxide-ionic conduction. The Sm- and Gd-doped samples have almost the same electrical conductivity. In this temperature range, an oxide-ionic conduction of these samples governs to the electrical conductivity, the values of the samples were 4.0 − 5.3 × 10^3 S/cm at 500°C and 1.4 − 1.8 × 10^2 S/cm at 600°C.

Figure 5 shows the differential coefficient of

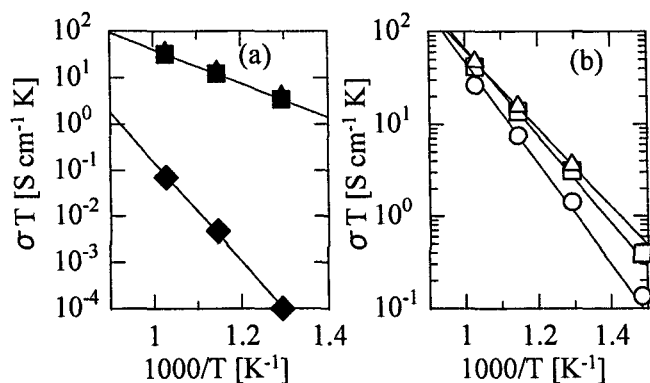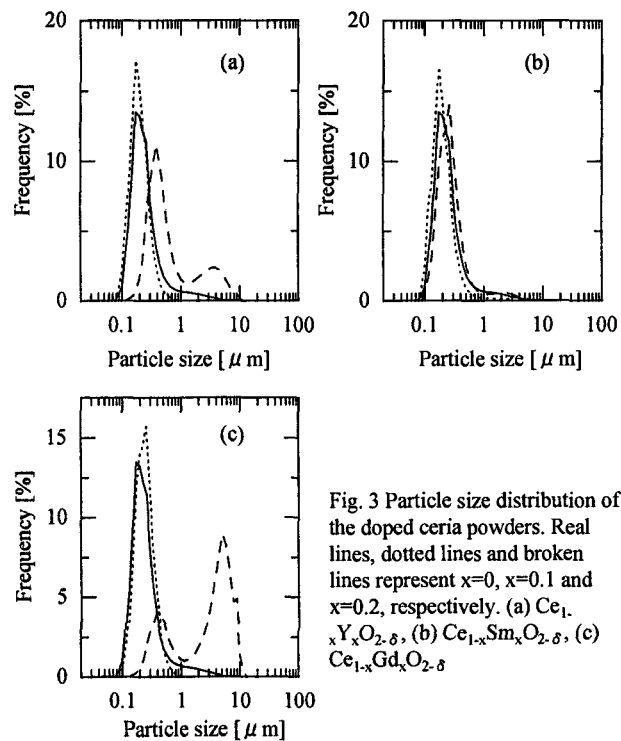Fig. 4 Arrhenius plots of ionic conductivity of $Ce_{1-x}RE_xO_{2-\delta}$ samples with relative density of approximately 95%. (◆) CeO_2; (▲) $Ce_{0.9}Sm_{0.1}O_{1.95}$; (■) $Ce_{0.9}Gd_{0.1}O_{1.95}$; (○) $Ce_{0.8}Y_{0.2}O_{1.9}$; (△) $Ce_{0.8}Sm_{0.2}O_{1.9}$; (□) $Ce_{0.8}Gd_{0.2}O_{1.9}$.
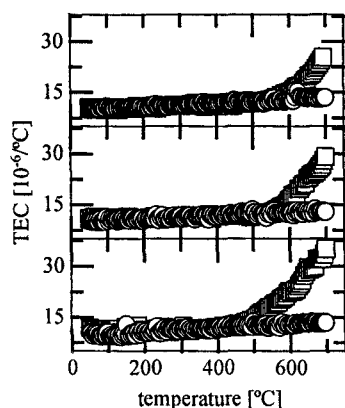
Fig.5 Differential coefficient of $Ce_{1-x}Gd_xO_{2-\delta}$. Open circles and open squares represent TECs in air and under H_2, respectively. (a) CeO_2: (b) $Ce_{0.9}Gd_{0.1}O_{1.95}$: (c) $Ce_{0.8}Gd_{0.2}O_{1.9}$.

thermal expansion-temperature curve of $Ce_{1-x}Gd_xO_{2-\delta}$, where the TECs are calculated using thermal expansion slops between 2.5°C above and 2.5°C below a give temperature. In air, all the samples showed a linear temperature dependence. On the other hand, TEC in H_2 atmosphere increased remarkably at around 500 - 600°C. This increase corresponds the reduced expansion. It is observed that the temperatures, where the reduced expansion of the samples starts, lower with increasing dopant content in the H_2 atmosphere, due to the formed oxygen vacancies and in a charge-compensating by oxidizing of Ce^{4+} to Ce^{3+} ions. Linear TEC and reduced temperatures of the samples in the present study were summarized in Table II.

4. CONCLUSION

The low-temperature sinterable RE-doped ceria powders have been synthesized through the heat-treatment process in the coprecipitation method. These powders show the lowest value in the reported sintering temperatures of rare earth metal-doped ceria powders. Electrical and thermal properties of these sintered samples were comparable to those of the ordinal coprecipitation method. Use of sintering aids is undesirable because such aids may damage other cell components. The present low-temperature sintering characteristics of the electrolyte without sintering aids are quite attractive in view of the problems associated with the low-temperature SOFC fabrication process. The results of this work will inspire the further developments of the SOFC.

REFERENCES
[1] K. Yamada and C-J. Wen, in Proceedings of Fifth European Solid Oxide Fuel Cell Forum, Edited by J. Huijsmans, ISBN 3-905592-10-X, 1-5 July 2002, Lucerne/Switzerland, (2002) p.1165
[2] H. Yashiro, Y. Eguchi, K. Eguchi, H. Arai, J. Appl. Electrochem. 18, 527(1988).
[3] M. Mori, T. Abe, H. Itoh, O. Yamamoto, Y. Takeda, and T. Kawahara, Solid State Ionics 74, 157(1994).
[4] E. Suda, B. Pacaud, Y. Montardi, M. Mori, M. Ozawa and Y. Takeda, Electrochemistry, 71 (10), p.866 (2003).
[5] For example, J. Van herle, T. Horita, T. Kawada, N. Sakai, H. Yokokawa and M. Dokiya, in Proceedings of the forth International Symposium on Solid Oxide Fuel Cells. Edited by M. Dokiya, O. Yamamoto, H. Tagawa, and S. C. Singhal, The Electrochemical Society, Pennington, NJ, Vol.95-1, (1995)p.1082.
[6] M. Mori, M. Yoshikawa, H. Itoh, and T. Abe, J. Am. Ceram. Soc., 77 (8), 2217(1994).
[7] M. Mori and N. M. Sammes, Solid State Ionics 146 301(2002).
[8] H. Hayashi, R. Sagawa, H. Inaba, and K. Kawamura, Solid State Ionics 131 281(2000).
[9] Y. Moriyoshi, T. Sasamoto, K. Uematsu, Y. Ikuma, H. Kadoma, T. Ikegami and T. Maruyama, "Sintering of Ceramics", Uchida Rokakuho Publishing Co., Ltd. ISBN 4-7536-5189-4 C3058, (1995).
[10] E. Lucchini and C. Schmid, J. Mater. Sci. Lett., 7, 523(1988).
[11] J. Bentzen, P. Husum and O. Soerensen, Mater. Sci. Monogr., 38, 385(1987).
[12] L. Moscardini D'Assuncao and I. Giolito, Thermochim. Acta, 137, 319(1989).
[13] R. Bevins, G. Rowbotham and F. Stephens, Am. Mineral., 70, 411(1985).
[14] B. C. H. Steele, Solid State Ionics 129, 95(2000).
[15] I. Yasuda and M. Hishinuma, in Proceedings of the Ionic and Mixed Conducting Ceramics III. Edited by T. A. Ramanarayanan, W. Worrell, H. L. Tuller, A. C. Khandkar, M. Mogensen, and W. Gopel, The Electrochemical Society, Pennington, Vol. 97-24, (1998)p.178.
[16] R. D. Shannon and C. T. Previtt, Acta Cryst., B25, 925 (1969).

Table II Linear thermal expansion coefficients and reduced temperatures of the sintered samples in the present study.

Sample	TEC ($\times 10^{-6}$°C)						Reduced expansion temperature (°C)
	50-500°C		50-600°C		50-700°C		
	air	H_2	air	H_2	air	H_2	
CeO_2	11.2	10.9	11.5	11.3	11.5	11.7	600
$Ce_{0.9}Y_{0.1}O_{1.95}$	11.2	11.3	11.4	11.7	11.4	11.7	600
$Ce_{0.8}Y_{0.2}O_{1.9}$	11.2	11.4	11.5	11.6	11.5	11.6	550
$Ce_{0.9}Sm_{0.1}O_{1.95}$	11.7	11.3	11.9	11.6	11.9	12.9	600
$Ce_{0.8}Sm_{0.2}O_{1.9}$	10.9	11.6	11.2	11.9	11.2	13.0	550
$Ce_{0.9}Gd_{0.1}O_{1.95}$	11.3	11.4	11.5	11.7	11.5	12.6	600
$Ce_{0.8}Gd_{0.2}O_{1.9}$	11.0	11.6	11.3	12.8	11.3	13.2	500